TU Delft

Delft University of Technology

Product shape selectivity of MFI-type, MEL-type, and BEA-type zeolites in the catalytic hydroconversion of heptane

Poursaeidesfahani, Ali; de Lange, Martijn F.; Khodadadian, Fatemeh; Dubbeldam, David; Rigutto, Marcello; Nair, Nitish; Vlugt, Thijs J.H.

DOI
10.1016/j.jcat.2017.07.005

Publication date
2017

Document Version
Final published version

Published in
Journal of Catalysis

Citation (APA)
Poursaeidesfahani, A., de Lange, M. F., Khodadadian, F., Dubbeldam, D., Rigutto, M., Nair, N., & Vlugt, T. J. H. (2017). Product shape selectivity of MFI-type, MEL-type, and BEA-type zeolites in the catalytic hydroconversion of heptane. *Journal of Catalysis*, *353*, 54-62. https://doi.org/10.1016/j.jcat.2017.07.005

Important note
To cite this publication, please use the final published version (if applicable).
Please check the document version above.

Copyright
Other than for strictly personal use, it is not permitted to download, forward or distribute the text or part of it, without the consent of the author(s) and/or copyright holder(s), unless the work is under an open content license such as Creative Commons.

Takedown policy
Please contact us and provide details if you believe this document breaches copyrights.
We will remove access to the work immediately and investigate your claim.

This work is downloaded from Delft University of Technology.
For technical reasons the number of authors shown on this cover page is limited to a maximum of 10.

Journal of Catalysis 353 (2017) 54–62

Contents lists available at ScienceDirect

Journal of Catalysis

journal homepage: www.elsevier.com/locate/jcat

Product shape selectivity of MFI-type, MEL-type, and BEA-type zeolites in the catalytic hydroconversion of heptane

Ali Poursaeidesfahani [a], Martijn F. de Lange [a], Fatemeh Khodadadian [b], David Dubbeldam [c], Marcello Rigutto [d], Nitish Nair [e], Thijs J.H. Vlugt [a,*]

[a] Engineering Thermodynamics, Process & Energy Department, Faculty of Mechanical, Maritime and Materials Engineering, Delft University of Technology, Leeghwaterstraat 39, 2628CB Delft, The Netherlands
[b] Process Intensification, Process & Energy Department, Faculty of Mechanical, Maritime and Materials Engineering, Delft University of Technology, Leeghwaterstraat 39, 2628CB Delft, The Netherlands
[c] Van't Hoff Institute for Molecular Sciences, University of Amsterdam, Science Park 904, 1098XH Amsterdam, The Netherlands
[d] Shell Global Solutions International, PO Box 38000, 1030BN Amsterdam, The Netherlands
[e] Shell India Markets Private Limited, Kundanahalli Main Road, Bangalore 560048, Karnataka, India

ARTICLE INFO

Article history:
Received 26 April 2017
Revised 27 June 2017
Accepted 5 July 2017
Available online 25 July 2017

Keywords:
Zeolites
Hydrocracking
Product distribution
Shape selectivity
Experiments
Molecular simulation

ABSTRACT

The influence of product shape selectivity on the bifunctional conversion of n-C_7 by zeolite catalysts is investigated. Three different zeolite catalysts with different pore sizes (MFI-type, MEL-type, and BEA-type zeolites) have been investigated experimentally. For all three catalysts, n-C_7 is isomerized to mono-branched isomers which are further isomerized into dibranched isomers, and these dibranched molecules are converted into cracking products. More dibranched isomers and less cracking products are produced by BEA-type zeolite compared to MFI-type and MEL-type zeolites and clear differences are observed in the distribution of dibranched isomers produced by different catalysts. Molecular simulation is used to compute the adsorption isotherms and free energy barriers for diffusion of dibranched isomers in MFI-type, MEL-type, and BEA-type zeolites. Combining simulation results and experimental observations, it is shown that product shape selectivity can explain the distribution of dibranched molecules while transition state shape selectivity fails to do so. For the medium-pore zeolites (MFI-type and MEL-type zeolites), free energy barriers for diffusion of dibranched molecules are significant. For MFI-type and MEL-type zeolites, the dibranched molecule that has to overcome lower diffusion barrier is produced with a higher yield and the distribution of dimethylpentane molecules is determined by their diffusion rate. It is shown that there is almost no free energy barrier for the diffusion of any of these molecules in BEA-type zeolite. As BEA-type zeolite imposes no free energy barrier for diffusion of any of dibranched isomers, the distribution of dibranched isomers is very close to the equilibrium distribution in the gas phase. Due to the limited mobility of dimethylpentanes within the pores of MFI-type and MEL-type zeolites, most of the dimethylpentane molecules are trapped inside the zeolite and undergo consecutive cracking. Dimethylpentane molecules diffuse sufficiently fast in the large pores of BEA-type zeolite and transfer to the gas phase, before consecutive reaction converts these molecules into cracking products. Moreover, the effect of the MFI-type crystal size on the production of dibranched isomers is investigated. The yield of dibranched isomers reduces by increasing the size of the crystal and larger part of dibranched isomers are cracked as the crystal size of MFI-type is increased.

© 2017 Elsevier Inc. All rights reserved.

1. Introduction

Zeolites are microporous materials which are extensively used as catalysts and adsorbents in the oil and gas industry since the late 1950s [1,2]. The remarkable stability and accessibility of their pores from the outside have made them interesting for many industrial applications [1,2]. Zeolite-based catalysts are crucial to the production of fuels, lubricants and petrochemicals, in oil refining and, increasingly, in gas to liquids (GTL) technology [3–6]. Conversion of linear hydrocarbons into branched ones increases the octane number of fuels and improves the performance of lubricants at low temperatures [7,8]. As a key example, a very large and steadily increasing fraction of todays clean transportation fuels

* Corresponding author.
E-mail address: t.j.h.vlugt@tudelft.nl (T.J.H. Vlugt).

http://dx.doi.org/10.1016/j.jcat.2017.07.005
0021-9517/© 2017 Elsevier Inc. All rights reserved.

is produced through zeolite-catalyzed hydrocracking, with a global capacity of over 500 million tons per annum. Another example is catalytic dewaxing of fuels and lubricants, which aims to achieve selective isomerization of alkanes or alkyl chains while minimizing hydrocracking reactions [8]. In these applications, catalytic activity, selectivity, and product quality all critically depend on the pore architectures of the zeolites. Due to the industrial importance of this process, many studies focused on hydroconversion of linear alkanes by zeolite catalysts. These include investigating the influence of zeolite crystal size and activity [4–6], comparison of performance of different zeolite catalysts [7–10], and the development of kinetic models [11–13]. The hydroconversion process of linear hydrocarbons can be seen as a chain of reactions [14,8,11,12,6,15]. First, linear hydrocarbons are adsorbed and subsequently dehydrogenation occurs at the metal sites of the catalyst form alkenes. These alkenes migrate to the acid sites where alkylcarbenium ions are formed through protonation. The alkylcarbenium ions can undergo isomerization and cracking. Finally, these resulting ions are transferred to acid sites where they are transformed into alkanes. Zeolite shape selectivity influences most of these steps and results in vastly different product distributions when different catalysts are used. There are basically three forms of shape selectivity [1,16]: *(1)* Reactant shape selectivity: Adsorption and/or diffusion of (some of the) reactant molecules to the reaction sites is inhibited by the confinement created by the zeolite pores. *(2)* Transition state shape selectivity: Formation of some products is hindered by the shape of the zeolites pores simply because they are too large to fit inside the pore structure. *(3)* Product shape selectivity: Diffusion limitations prohibit desorption of some product molecules that are too bulky to diffuse sufficiently fast along the channels of the zeolite. If the reactants have limited mobility they will stay longer at the active sites and the probability for the consecutive reactions to take place and convert these molecules is increased [17,1,16,18]. Due to the complexity of the aforementioned reaction mechanism, it is particularly difficult to study the influence of different forms of shape selectivity on individual steps of the hydroconversion process. During the past decades, a significant number of studies tried to improve the understanding of the shape selective behavior of zeolite catalysts in bifunctional conversion of alkanes [19–21,9,7,22]. Whereas concepts of shape selectivity in zeolite catalysis have been very useful in qualitatively explaining product distributions based on differences in pore geometry [7,9] and in assisting catalyst development in a qualitative fashion, quantitative treatments of reaction kinetics in shape selective reactions allowing unambiguous interpretation of shape selectivity in terms of reactant selectivity, transition state, and product shape selectivity have been scarce [23,24]. Recent advancements in computing power have made molecular simulation a powerful tool to provide fundamental information regarding the adsorption and diffusion properties of reactants and products at the molecular scale [25–29]. It is now possible to compute adsorption isotherms, spatial distributions, and free energy landscapes of the reactant and product molecules within the pore network of zeolites [30,1,17]. From both scientific and applied perspective, such treatments should eventually aim for quantitative predictions. In this paper, a quantitative treatment of competitive adsorption and diffusion of reactants and products is presented in a very relevant model reaction: the hydroisomerization/hydro cracking of n-heptane by three zeolite catalysts (BEA-type, MFI-type, and MEL-type zeolites). The results are combined with experimental observations and used to explain trends in the reaction kinetics, as a step towards a full quantitative treatment.

This paper is organized as follows. In Section 2, molecular simulations methods and simulation details used to compute adsorption isotherms and free energy landscapes of reactants and product molecules are described. Experimental details are provided in Section 3. The product distributions obtained with different catalysts and crystal sizes (for MFI-type) are discussed in details in Section 4. Our main findings are summarized in Section 5.

2. Simulations

The adsorption isotherms and free energy profiles of different heptane isomers are computed using force field based Monte Carlo Simulations. Adsorption isotherms show the strength of adsorption of different components and can be directly used to study transition state shape selectivity. Free energy profile shows the relative free energy of a molecule as a function of its location inside channels. The free energy landscape of reactant and product molecules within the pores of the zeolite show the mobility of these molecules inside the zeolites can be used in more quantitative investigation of product shape selectivity of zeolite catalysts. The RASPA software package is used for the simulations [31]. Heptane isomers are modeled using the TraPPE force field [32,33]. A cutoff radius of 12 Å is applied for for Lennard-Jones interactions and no tail corrections are used. The simulation box consists of $2 \times 2 \times 1$ rigid unit cells for BEA-type zeolite and $2 \times 2 \times 2$ for MFI-type and MEL-type zeolites with periodic boundary conditions. Zeolite structure were taken from the IZA database [34]. Adsorption isotherms are obtained by performing simulations in the grand-canonical ensemble at $T = 227\ ^\circ$C and $T = 303\ ^\circ$C. At each Monte Carlo step of grand-canonical simulations an attempt is made to either displace, regrow, rotate, insert, or remove a randomly chosen hydrocarbon chain. Hydrocarbon chains are regrown/inserted using the Congurational-Bias Monte Carlo (CBMC) technique [35–38]. The free energy profile of different heptane isomers along the channels of these structures at zero loading are computed from Monte Carlo simulations in the canonical ensemble. The length of the channels are divided into 1000 slices and the probability of being in each of these slices is calculated using only a single molecule. To compute the free energy profiles along a channel, the possible positions for the molecule are restricted to a single channel and trial moves attempting to move the molecule outside the channel are automatically rejected. The free energy of the molecule at each slice is given by:

$$F_i = -k_B T \ln p_i \tag{1}$$

where T is the temperature, k_B is the Boltzmann factor, and F_i and p_i are the average free energy at slice i and the probability of molecule being in slice i, respectively. The free energy profile can have very low local minima. When the molecule reaches these local minima, the energy penalty for the trial move that transfers the molecule out of local minima would be very high. Therefore, these translational trial moves are rarely accepted. This results in very poor sampling of the configurations in which the molecules is not in local minima. To improve the sampling, a biasing factor ($\exp[w_i]$) is added to statistical weight for each slice [39]. These biasing factors are computed iteratively so that the observed probability for the molecule being in any of the slices is the same. In this case, the free energy of the molecule at each slice is given by:

$$F_i = -k_B T(\ln p_i - w_i) \tag{2}$$

The RASPA software is used for simulations [31,40]. More details regarding the simulations techniques can be found elsewhere [41,17].

3. Experiments

Three samples of zeolite MFI-type were used with different crystal sizes: (1) a large-crystal material (denoted by MFI-bulk) with composition Si/Al = 20 and BET surface area 373 m^2/g (crys-

tals of about 1 μm) described by Zhu et al. [42]; (2) CBV-8014G, a commercial MFI-type (denoted by MFI-reference) with Si/Al = 40 and BET surface area of 425 m^2/g consisting of aggregates of 40–150 nm primary crystals, obtained from Zeolyst International; (3) a MFI-type nanosheet material (denoted by MFI nanosheet) with Si/Al = 20 and approximately 20 nm long and 4 nm thick sheets, described by Zhu et al. [42] (sample ZMS-5-F(3,20,423)). Samples of zeolite BEA-type with Si/Al = 50 BET and a surface area of 700 m^2/g and a crystal size of approximately 400 nm and of MEL-type with Si/Al = 23 and BET surface area of 440 m^2/g (crystal sizes ranging from 100–200 nm) were also obtained from Zeolyst International. The crystal size of the MFI-bulk is much larger than the MFI nanosheet and MFI-reference, and the crystal size of the MEL-type is sufficiently small and of the same order as BEA-type and MFI-reference. All three structure are formed by three-dimensional pore networks. The pore network of BEA-type zeolite is formed by 12-membered-rings straight pores while the pore networks of MFI-type and MEL-type zeolites contain 10-membered-rings.

Hydroconversion of heptane was carried out on Pd-loaded zeolites as described previously [43]. The dried support was shaped in a sieve fraction (177–420 μm) and loaded with 0.4 wt% Pd via incipient wetness impregnation with a solution of appropriate concentration of $Pd(NH_3)_4(NO_3)_2$. The resulting materials were calcined at 300 °C. Prior to testing, the catalysts were reduced at 320 °C at 30 bar in flowing hydrogen. Hydroconversion of n-heptane was carried out at 30 bar using 300 mg of catalyst and H_2/hydrocarbon ratio of 24 mol/mol. Experiments are conducted in a flow reactor and the flow rate of hydrogen is set to 25 ml min^{-1}. To investigate various conversion levels (5–95%), the reaction temperature was lowered from 320 °C to 200 °C at a rate of 0.2 °C min^{-1}, and products were analyzed by online GC.

4. Results and discussion

4.1. Reaction scheme and production of dibranched isomers

For all catalysts, normal C_7 is transformed into monobranched isomers (M), multibranched isomers (T), and cracking products (C). No secondary cracking is observed in this temperature range (200–320 °C) and the only observed cracking products are i-C_4, n-C_4, and C_3. The monobranched isomers mainly consist of methylhexanes. The fraction of ethylpentane in total monobranched isomers was lower than 5% for all catalysts and for all conversion levels. No traces of trimethylbutane were detected for MFI-type and MEL-type zeolites, and for BEA-type zeolite, less than 1% of heptane is converted to trimethylbutane. In Fig. 1, the yields of monobranched isomers (M) and multibranched isomers (T) and cracking products (C) are shown as a function of the conversion of n-C_7. It can clearly be seen that the monobranched isomers are the primary reaction products and cracking products and multibranched isomers are secondary reaction products. Heptane isomers are consecutively cracked to either i-$C_4 + C_3$ or n-$C_4 + C_3$. Cracking of monobranched isomers exclusively produces n-$C_4 + C_3$, while cracking of most of the multibranched isomers (except 23-dimethylpentane) results in production of i-$C_4 + C_3$. Therefore, the i-C_4/n-C_4 ratio indicates whether monobranched or multibranched isomers are the main reactants in the cracking reactions. The i-C_4/n-C_4 ratio is larger than 15 for all the catalysts and for the entire conversion range. This shows that the main reaction scheme for the hydroconversion of n-C_7 on all three catalysts is:

$$\text{n-}C_7 \rightleftharpoons M \rightleftharpoons D \rightarrow \text{i-}C_4 + C_3 \qquad \text{(Reaction.1)}$$

Methylhexanes and dimethylpentanes have by far the highest share in the produced monobranched and multibranched isomers, respectively. In Fig. 2a and b, the yields of methylhexanes and dimethylpentanes for the three catalysts are compared for the entire range of n-C_7 conversion, respectively. The yield of methylhexanes for the three zeolites are almost the same, regardless of the conversion level. BEA-type zeolite produces slightly less methylhexanes compared to MFI-type and MEL-type zeolites in the conversion range (60–80%). However, these catalysts behave very differently while considering the production of dimethylpentanes (Fig. 2b). BEA-type zeolite has by far the highest rate of production for dimethylpentanes.

The experimental data presented in Fig. 3 shows the ratio between the yield of dimethylpentanes and i-C_4. Considering the main reaction scheme (Reaction.1), this ratio essentially mimics the ratio of dimethylpentanes that transferred to the gas phase to dimethylpentanes which are cracked to i-$C_4 + C_3$ and then transferred to the gas phase. It is clear that this ratio is always larger than one for BEA-type zeolite and larger than 3 in the conversion range (10–80%). This means that on average three out of four dimethylpentane molecules that are formed in BEA-type zeolite are transferred into the gas phase, and only one is cracked. This shows that most of the dimethylpentanes that are produced in BEA-type zeolite can leave the structure before undergoing cracking into i-C_4. However, the ratio between the yield of dimethylpentanes and i-C_4 is always lower than one (around 0.1) for MFI-type and MEL-type zeolites. This means that on average nine out of ten dimethylpentane molecules that are formed in MFI-type and MEL-type zeolites are cracked and only one is transferred into the gas phase. This suggests that diffusion rate for dimethylpentane molecules is much higher in channels of BEA-type zeolite compared to that of MFI-type and MEL-type zeolites. To validate this argument, one should have knowledge on the diffusion of different heptane isomers within these three catalysts. This is achieved by computing the free energy profiles of different heptane isomers along the channels of the three structures. MEL-type and BEA-type zeolites have only single type of straight channels in two perpendicular directions while MFI-type has two types of channels straight and zigzag in two perpendicular directions. In Fig. 4, the free energy profiles of different heptane isomers in the straight channels of MFI-type, MEL-type, and BEA-type zeolites are shown. When considering diffusion, only the relative free energies as a function of the position along the channels are important. Therefore, the free energy profiles shown in Fig. 4 are shifted in such a way that the minimum of free energy is always zero. The free energy barrier for diffusion can be defined as the difference between the maximum and minimum of the free energy profiles. These values are listed in Table 1. It is clear that there is almost no free energy barrier for diffusion of all heptane isomers in large pores of BEA-type zeolite (see Fig. 5). The free energy barriers of different heptane isomers in MFI-type and MEL-type zeolites are 2-methylhexane $\approx$ 3-methylhexane $<$ 24-dimethylpentane $<$ 23-dimethylpentane $\ll$ 22-dimethylpentane $\approx$ 33-dimethylpentane. Therefore, due to the absence of any considerable free energy barrier for diffusion of dimethylpentane molecules in BEA-type zeolite, most of dimethylpentane molecules can move to the gas phase before cracking. However, in MFI-type and MEL-type zeolites, dimethylpentane molecules must overcome significant free energy barriers before they can move to the gas phase. Therefore, most of the dimethylpentane molecules that are produced in MFI-type and MEL-type zeolites are trapped inside the zeolite and cannot diffuse to the gas phase. Dimethylpentane molecules are more likely to undergo cracking and form i-$C_4 + C_3$ which can diffuse out of the zeolite much faster than dimethylpentane molecules. This also explains why BEA-type zeolite has a higher production rate for

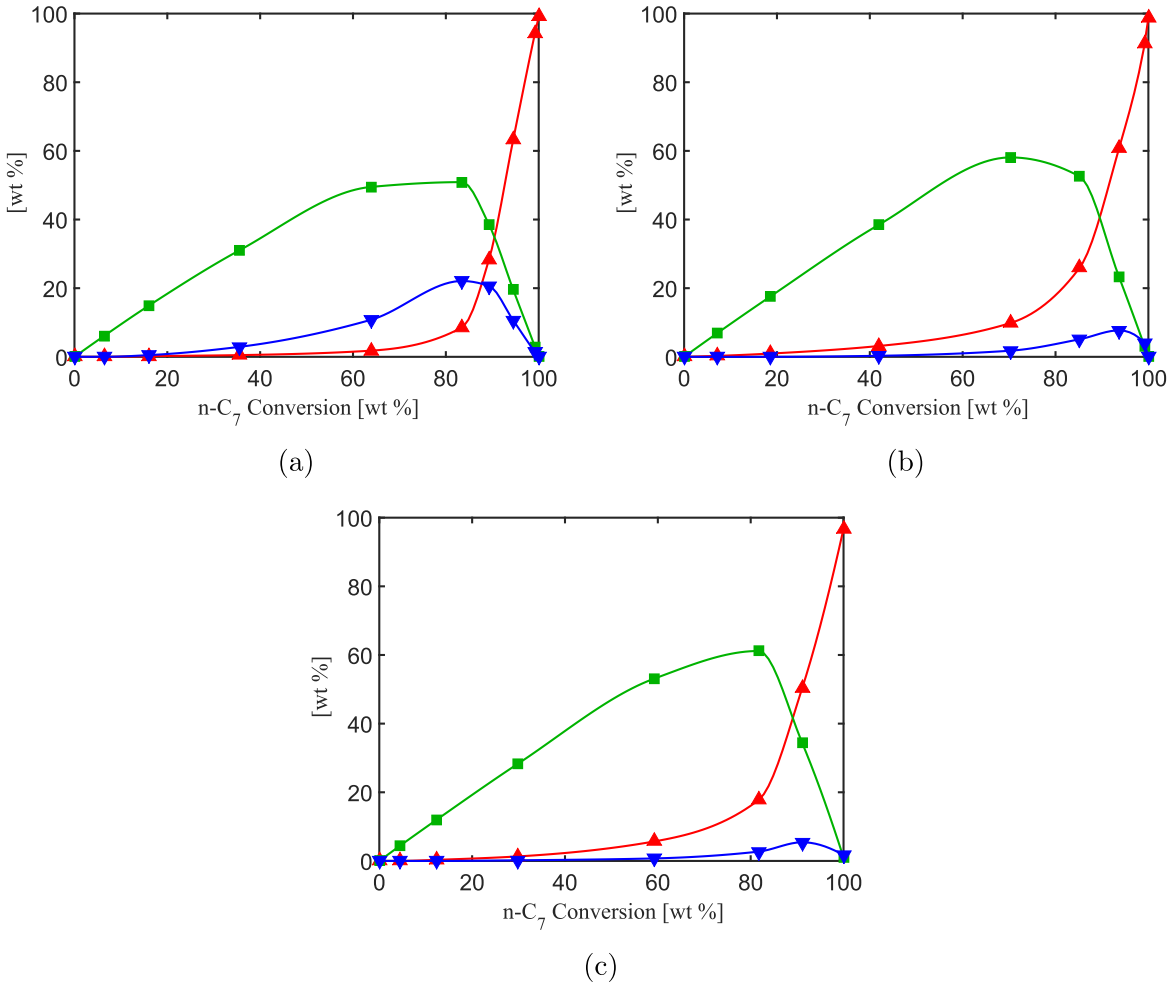

Fig. 1. The experimental yields of monobranched isomers (green □) and multibranched isomers (blue ▽) and cracking products (red △) are plotted as a function of the conversion of n-C_7 for (a) BEA, (b) MFI, and (c) MEL. Different conversion levels are obtained by changing the temperature of the reactor between 200 °C and 320 °C. Lines are a guide to the eye.

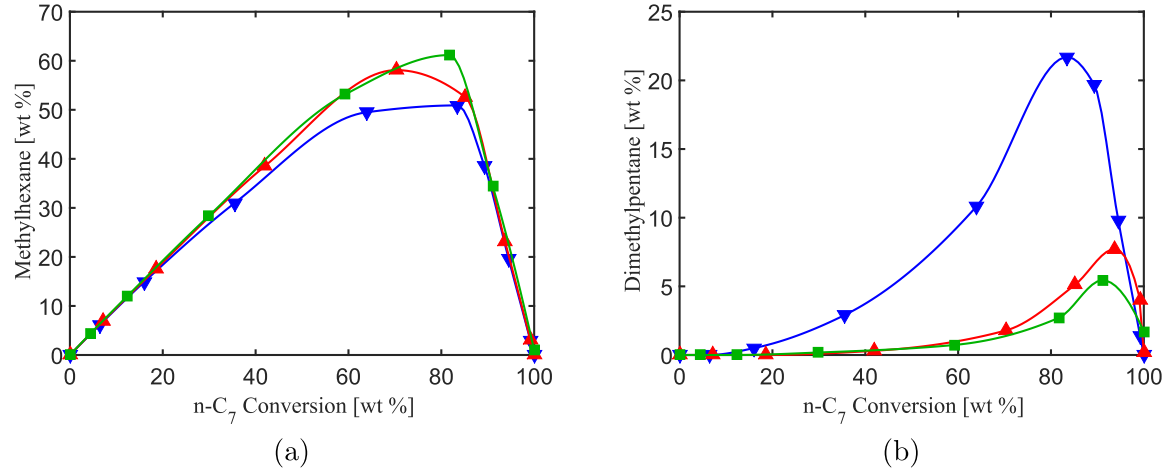

Fig. 2. The experimental yields of (a) methylhexane and (b) dimethylpentane are plotted as a function of the conversion of n-C_7 for BEA (blue ▽), MFI (red △), and MEL (green □). Different conversion levels are obtained by changing the temperature of the reactor between 200 °C and 320 °C. Lines are a guide to the eye.

dimethylpentanes. The difference between BEA-type zeolite and the other two zeolites is that in BEA-type zeolite dimethylpentanes can move to the gas phase. Moreover, the channels of BEA-type zeolite are large enough so that dimethylpentane molecules can be formed almost anywhere inside the structure. However, dimethylpentane molecules can only fit within the intersections of MFI-type and MEL-type zeolites [30] (see Fig. 5). As a result, in the case of BEA-type zeolite, more dimethylpentane molecules

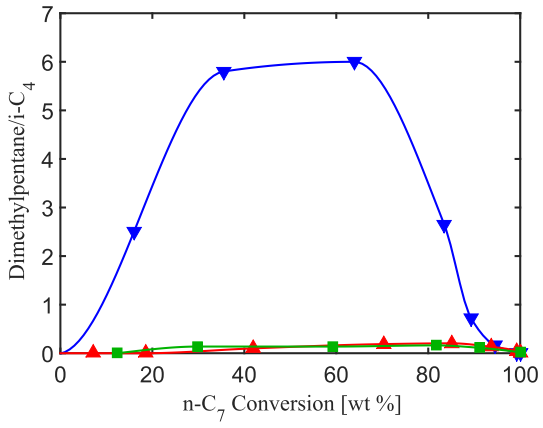

Fig. 3. The ratio between the yield of dimethylpentanes and i-C_4 plotted as a function of the conversion of n-C_7 BEA (blue ▽), MFI (red △), and MEL (green □). Different conversion levels are obtained by changing the temperature of the reactor between 200 °C and 320 °C. Lines are a guide to the eye.

are produced and more methylhexanes are consumed compared to the cases of MFI-type and MEL-type zeolites. Therefore, as in the case in Fig. 2a, one would expect to have lower concentration of monobranched isomers when BEA-type zeolite is used as a catalyst.

4.2. Distribution of dibranched isomers

Dimethylpentanes with geminal methyl groups (22,33-dimethylpentane) have very high free energy barriers for diffusion in the channels of MFI-type and MEL-type zeolites (see Table 1 and Fig. 4). This suggests that dimethylpentanes with the geminal methyl groups can only fit within the intersections of the two channels (where free energy is minimal). Hence, it is almost impossible for these molecules to move to the gas phase. Therefore, they are trapped inside the intersections until they are cracked. Among all dimethylpentanes, 24-dimethylpentane has the lowest free energy barrier for diffusion. The free energy barrier for the diffusion of 24-dimethylpentane is closer to that of the methylhexanes than to the other dimethylpentanes. Therefore, it is expected that the yield of dimethylpentanes obtained from MFI-type and MEL-type zeolites predominantly consists of 24-dimethylpentane. The yields of different dimethylpentane isomers as a function of the conversion of n-C_7 for the three structures are shown in Fig. 6. It can be seen that 24-dimethylpentane is the most produced dimethylpentane on MFI-type and MEL-type zeolites, followed by 23-dimethylpentane. This is exactly what is expected from the analysis of the free energy profiles. The fastest diffusing dimethylpentane (the one with the lowest free energy barrier) has the largest share in the total production of dimethylpentanes. As shown in Fig. 4 and Table 1, free energy barriers of all heptane isomers are higher and the differences between them are more significant in the straight pores of MEL-type compared to straight pores of MFI-type. This can explain the higher yield of dimethylpentanes on MFI-type. For BEA-type zeolite, 23-dimethylpentane has the highest yield among dimethylpentanes for the entire conversion range of n-C_7 (see Fig. 6). The yield of 22-dimethylpentane and 24-dimethylpentane are almost the same for all conversions and 33-dimethylpentane has always the lowest fraction among dimethylpentanes. Interestingly, the fraction of different dimethylpentanes in the total dimethylpentanes produced remains roughly constant and corresponds to the equilibrium distribution of dimethylpentanes in the gas phase. From the free energies of formation of different dimethylpentanes, one can compute

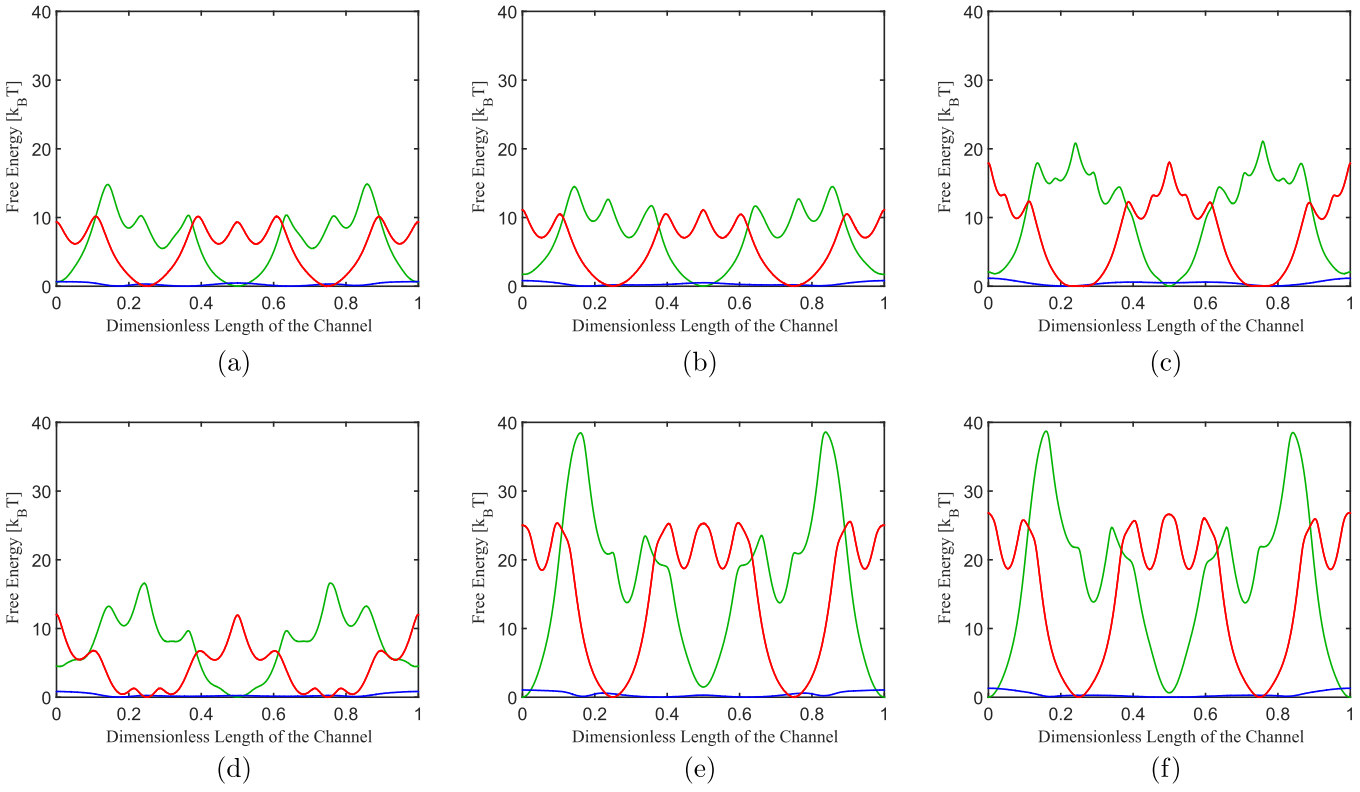

Fig. 4. The free energy profiles of (a) 2-methylhexane, (b) 3-methylhexane, (c) 23-dimethylpentane, (d) 24-dimethylpentane, (e) 22-dimethylpentane, (f) 33-dimethylpentane at zero loading are plotted as a function of the position of the molecule in straight channels of for BEA (Blue), MFI (Red), and MEL (Green) at $T = 227$ °C. The free energy profiles are shifted in such a way that the minimum of free energy is always zero.

Table 1
Free energy barriers for diffusion of different heptane isomers in straight channels of MFI, MEL, and BEA-type zeolites at zero loading and at 227 °C, as computed by CBMC simulations.

Molecule	Free energy barrier/ [k_BT]		
	BEA	MFI	MEL
2-Methylhexane	0.68	10.2	14.9
3-Methylhexane	0.82	11.1	14.5
23-Dimethylpentane	1.17	18.0	21.1
24-Dimethylpentane	0.85	12.0	16.6
22-Dimethylpentane	1.06	25.6	38.6
33-Dimethylpentane	1.32	26.8	38.7

the equilibrium constants for the methyl-shift reactions in the gas phase:

$$K_{eq} = \exp\left[\frac{-\Delta G^{\circ}}{RT}\right] \quad (3)$$

where ΔG° is the Gibbs free energy of the reaction which is obtained by subtracting the Gibbs free energy of formation of products from those of reactants. The values for the Gibbs free energies of formation of heptane isomers reported by D.W. Scott [44] are used to compute the equilibrium constants for the methyl-shift reactions of dimethylpentanes in the gas phase. These values are shown in Table 2. The equilibrium distribution of dimethylpentanes and the distribution of dimethylpentanes produced by BEA-type zeolite are shown in Table 2. As BEA-type zeolite imposes no free energy barrier for diffusion of any of the dimethylpentanes and the methyl-shift reaction are very fast compare to isomerization reactions [8,6], the distribution of dimethylpentanes by BEA-type zeolite is equilibrium limited.

To investigate the influence of transition state shape selectivity, the adsorption isotherms of different dibranched isomers are studied. One should be cautious to use equilibrium adsorption isotherms to study the transition-state shape selectivity. The main assumption here is that the transition-state and product have almost the same shape, size and interactions with the zeolite structure. For the isomerization reactions, this assumption is not far from reality [1,16]. Dibranched molecules that fit better within the channels and intersections of a structure should have a higher loading. Those isomers with a lower loading fit more difficultly inside the pore network of the zeolite and, according to transition state shape selectivity, have lower probability of formation [1,16]. In Fig. 7, the adsorption isotherms of 23-dimethylpentane, 24-dimethylpentane, 22-dimethylpentane, and 33-dimethylpentane at $T = 227$ °C and $T = 303$ °C are shown for the three zeolite catalysts. For the entire pressure range, 24-dimethylpentane has the lowest loading in MFI-type (Fig. 7b), and still 24-dimethylpentane is the dibranched molecule that is preferentially produced. One can argue that a molecule which is weakly adsorbed by the catalyst has higher mobility compared to strongly adsorbed molecules and desorbs faster. As shown for MEL-type in Fig. 7c, 24-dimethylpentane has the highest loading at the pressure range of the experiments. However, this molecule is still produced with the highest concentration among all dimethylpentanes by MEL-type. While following the above argument, one would expect 24-dimethylpentane to have limited contribution in production of dimethylpentanes by MEL-type, due to the preferential adsorption of 24-dimethylpentane and consequently its lower tendency for desorption. Moreover, 22-dimethylpentane which is adsorbed preferentially by MFI-type and MEL-type zeolite has one of the lowest fractions in produced dimethylpentanes by these structures. This clearly shows that although the effect of adsorption strength can be interpreted in different ways, neither of these interpretations can explain the distribution of dimethylpentanes for these three catalysts. Therefore, transition state shape selectivity is not the underlying reason for the sharp difference between the distributions of dimethylpentanes in these three structures. The product shape selectivity can explain the difference between the distributions of dimethylpentanes very well. For MFI-type and MEL-type zeolites, the free energy barriers that different

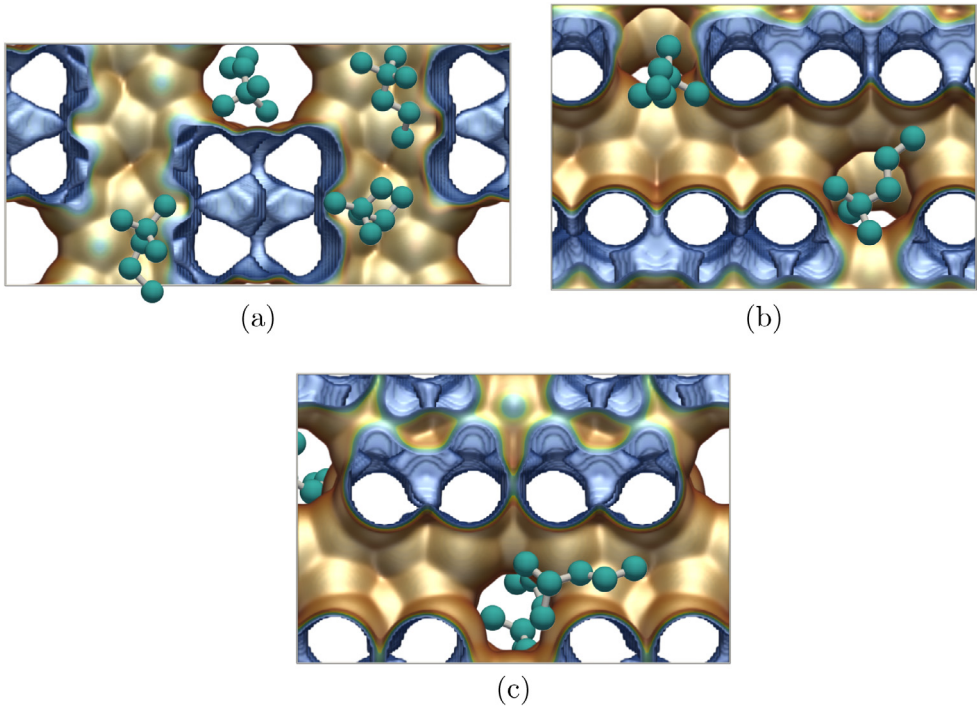

Fig. 5. Visualization of 22-dimethylpentane molecules within the pore structure of zeolite (a) BEA, (b) MFI, and (c) MEL. 22-dimethylpentane molecules can be everywhere within the pore structure of BEA. However, in pore structures of MFI and MEL, 22-dimethylpentane molecules are mostly at the intersection and only very rarely at the middle of the channels.

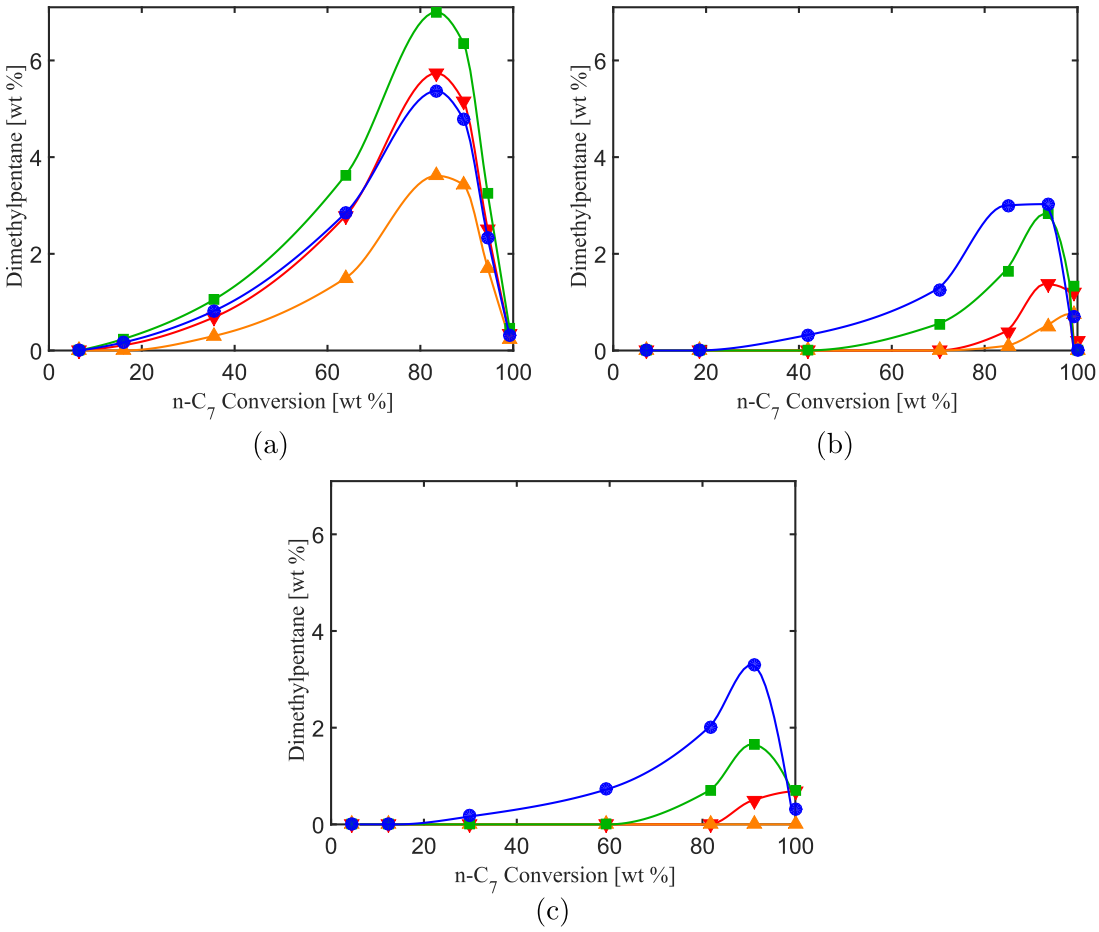

Fig. 6. The experimental yields of dimethylpentanes are plotted as a function of the conversion of n-C_7 for (a) BEA, (b) MFI, and (c) MEL. 23-dimethylpentane (green □), 24-dimethylpentane (blue ○), 22-dimethylpentane (red ▽), and 33-dimethylpentane (orange △). Different conversion levels are obtained by changing the temperature of the reactor between 200 °C and 320 °C. Lines are a guide to the eye.

Table 2
Equilibrium distribution of dimethylpentanes in the gas phase and the distribution of dimethylpentanes produced by BEA-type zeolite. The equilibrium distribution in the gas phase is obtained from the free energies of formation of dimethylpentanes at the mean temperature of the experiments (260 °C). The values for the Gibbs free energies of formation of heptane isomers reported by D.W. Scott [44] are used to compute the equilibrium distribution of dimethylpentanes in the gas phase. Numbers in brackets are uncertainties in the last digit, i.e., 0.25 (2) means 0.25 ± 0.02.

	Equilibrium (gas phase)	Produced by BEA
22-dimethylpentane	0.25(2)	0.26(1)
24-dimethylpentane	0.24(2)	0.25(1)
23-dimethylpentane	0.35(2)	0.32(1)
33-dimethylpentane	0.17(2)	0.16(2)

dimethylpentanes molecules need to overcome to reach the gas phase are significantly different. For these catalysts, the dibranched molecule that has to overcome lower diffusion barrier is produced with a higher yield. Channels of BEA-type zeolite are large enough that practically do not impose any free energy barrier for diffusion of any of the dibranched molecules. Therefore, in this case there is no product shape selectivity and the distributions of dimethylpentanes molecules can reach the equilibrium distribution in the gas phase.

4.3. MFI-type with different crystal sizes

The observations from the previous subsections suggest that product shape selectivity is the dominant form of shape selectivity in distribution of dimethylpentanes obtained from conversion of n-C_7 by MFI-type. It is shown that dimethylpentanes have a limited mobility inside the pore network of MFI-type. Therefore, one would expect that by increasing the crystal size dimethylpentane molecules are forced to stay longer inside the structure and in proximity of active sites. This increases the probability of consecutive cracking reactions to take place and convert these molecules to cracking products which can diffuse faster through the pores of MFI-type. Consequently, the yield of dimethylpentanes is expected to reduce by increasing the crystal size of MFI-type. To support the claims and arguments made in the previous sections, experiments have been conducted on three samples of zeolite MFI-type with different crystal sizes: (1) a large-crystal material (denoted by MFI-bulk) with composition Si/Al = 20 and BET surface area 373 m^2/g described by Zhu et al. [42]; (2) CBV-8014G, a commercial MFI-type with Si/Al = 40 and BET surface area of 425 m^2/g consisting of aggregates of 40–150 nm primary crystals, obtained from Zeolyst International; (3) a MFI-type nanosheet material (denoted by MFI nanosheet) with Si/Al = 20 and approximately 20 nm long and 4 nm thick sheets, described by Zhu et al. [42] (sample ZMS-5-F(3,20,423)). In Fig. 8, it can be seen that by increasing the crystal size, the production of dimethylpentanes and the ratio of produced dimethylpentanes to the cracking products decrease. Similar observations have been reported by other groups [45]. This is along the same lines with the previous observations and shows that diffusion of dimethylpentanes (product shape selectivity) has significant influence on the product distribution of n-C_7 conversion, when MFI-type is used as catalyst.

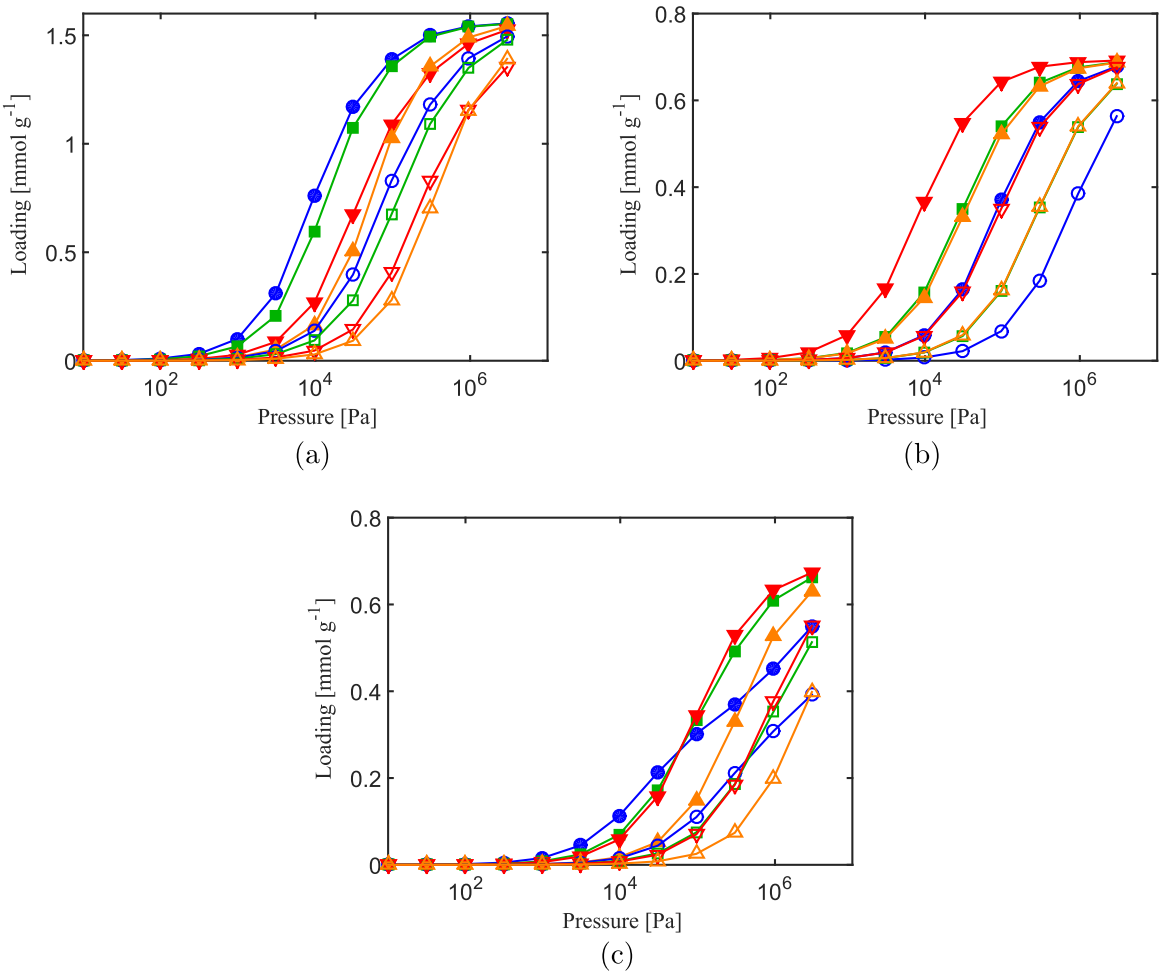

Fig. 7. The adsorption isotherms of 23-dimethylpentane (green □), 24-dimethylpentane (blue ○), 22-dimethylpentane (red ▽), and 33-dimethylpentane (orange △) at $T = 227$ °C (close symbols) and at $T = 303$ °C (open symbols) as computed with CBMC simulations. (a) BEA, (b) MFI, and (c) MEL. Lines are a guide to the eye.

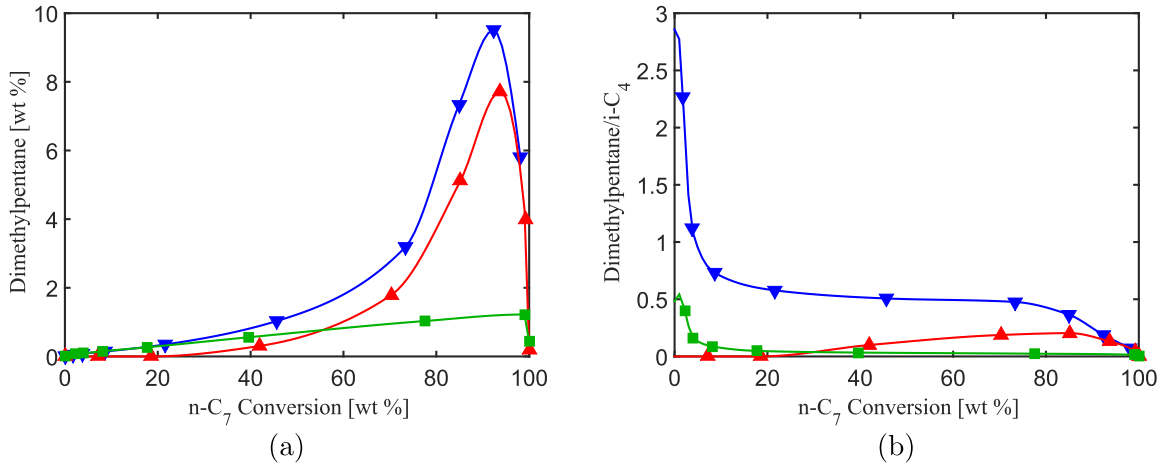

Fig. 8. The experimental yields of (a) dimethylpentane and (b) the ratio between the yield of dimethylpentanes and i-C_4 are plotted as a function of the conversion of n-C_7 for MFI nanosheet (blue ▽), MFI reference (red △), and MFI bulk (green □). Different conversion levels are obtained by changing the temperature of the reactor between 200 °C and 320 °C. Lines are a guide to the eye.

5. Conclusions

For all catalysts investigated in this study, n-C_7 is first converted into monobranched isomers. Monobranched isomers are further isomerized to dibranched isomers, and dibranched isomers are the main reactants for the cracking reactions. The free energy barriers for diffusion of different heptane isomers in MFI-type and MEL-type zeolites are orderd as 2-methylhexane ≈ 3-methylhexane < 24-dimethylpentane < 23-dimethylpentane ≪ 22-dimethylpentane ≈ 33-dimethylpentane. Significant free energy

barriers for diffusion of dibranched isomers in MFI-type and MEL-type zeolites inhibit transfer of these molecules to the gas phase. Therefore, most of the formed dibranched isomers remain inside the zeolite until they are cracked and fast diffusing cracking products are transferred to the gas phase. For MFI-type and MEL-type zeolites, the dibranched molecule that has to overcome lower diffusion barrier is produced with a higher yield. Clearly showing the importance of product shape selectivity for these catalysts, the shares of different dimethylpentane molecules in the total production of dibranched isomers are ordered as 24-dimethylpentane > 23-dimethylpentane ≫ 22-dimethylpentane ≈ 33-dimethylpentane. BEA-type zeolite catalyst showed the highest selectivity towards production of dibranched isomers. The free energy barriers computed for heptane isomers at zero loading show that all heptane isomers can diffuse through the large pores of BEA-type zeolite without encountering diffusion barriers. As BEA-type zeolite imposes no free energy barrier for diffusion of any of the dimethylpentanes, the distribution of dimethylpentanes by BEA-type zeolite is equilibrium limited. It can be concluded that product shape selectivity is the main source of sharp differences between the product distribution of BEA-type zeolite compared to MFI-type and MEL-type zeolites. The influence of product shape selectivity on distribution of dibranched products increases as the pore size decreases from almost no effect for BEA-type zeolite (equilibrium distribution) to completely dominant for MFI-type and MEL-type zeolites.

Acknowledgments

This work was sponsored by NWO Exacte Wetenschappen (Physical Sciences) for the use of supercomputer facilities, with financial support from the Nederlandse Organisatie voor Wetenschappelijk Onderzoek (Netherlands Organization for Scientific Research, NWO). The authors also gratefully acknowledge financial support from Shell Global Solutions B.V., and the Netherlands Research Council for Chemical Sciences (NWO/CW) through a VIDI grant (David Dubbeldam) and a VICI grant (Thijs J.H. Vlugt).

References

[1] B. Smit, T.L.M. Maesen, Chem. Rev. 108 (2008) 4125–4184.
[2] J. Jae, G.A. Tompsett, A.J. Foster, K.D. Hammond, S.M. Auerbach, R.F. Lobo, G.W. Huber, J. Catal. 279 (2011) 257–268.
[3] S. Sadrameli, Fuel 140 (2015) 102–115.
[4] A.A. Rownaghi, F. Rezaei, J. Hedlund, Chem. Eng. J. 191 (2012) 528–533.
[5] H. Konno, T. Okamura, T. Kawahara, Y. Nakasaka, T. Tago, T. Masuda, Chem. Eng. J. 207 (2012) 490–496.
[6] J.F. Denayer, J.A. Martens, P.A. Jacobs, J.W. Thybaut, G.B. Marin, G. Baron, Appl. Catal. A 246 (2003) 17–28.
[7] A. Soualah, J.-L. Lemberton, L. Pinard, M. Chater, P. Magnoux, K. Moljord, Appl. Catal. A 336 (2008) 23–28.
[8] C. Bouchy, G. Hastoy, E. Guillon, J. Martens, Oil & Gas Scie. Tech. 64 (2009) 91–112.
[9] J. Martens, R. Parton, L. Uytterhoeven, P. Jacobs, G. Froment, Appl. Catal. 76 (1991) 95–116.
[10] J.A. Swisher, N. Hansen, T. Maesen, F.J. Keil, B. Smit, A.T. Bell, J. Phys. Chem. C 114 (2010) 10229–10239.
[11] J.W. Thybaut, G.B. Marin, Chem. Eng. Technol. 26 (2003) 509–514.
[12] G. Martens, G. Marin, J. Martens, P. Jacobs, G. Baron, J. Catal. 195 (2000) 253–267.
[13] M. Steijns, G.F. Froment, Ind. Eng. Chem. Prod. Res. Dev. 20 (1981) 660–668.
[14] G.D. Svoboda, E. Vynckier, B. Debrabandere, G.F. Froment, Ind. Eng. Chem. Res. 34 (1995) 3793–3800.
[15] J. Thybaut, G. Marin, G. Baron, P. Jacobs, J. Martens, J. Catal. 202 (2001) 324–339.
[16] B. Smit, T.L. Maesen, Nature 451 (2008) 671–678.
[17] T.L.M. Maesen, M. Schenk, T.J.H. Vlugt, B. Smit, J. Catal. 203 (2001) 281–291.
[18] C.R. Marcilly, Top. Catal. 13 (2000) 357–366.
[19] J.F. Denayer, G.V. Baron, G. Vanbutsele, P.A. Jacobs, J.A. Martens, Chem. Eng. Sci. 54 (1999) 3553–3561.
[20] M.A. Baltanas, G.F. Froment, Comput. Chem. Eng. 9 (1985) 71–81.
[21] M.C. Claude, J.A. Martens, J. Catal. 190 (2000) 39–48.
[22] A. Janda, B. Vlaisavljevich, L.-C. Lin, S. Mallikarjun Sharada, B. Smit, M. Head-Gordon, A.T. Bell, J. Phys. Chem. C 119 (2015) 10427–10438.
[23] A. Janda, B. Vlaisavljevich, L.-C. Lin, B. Smit, A.T. Bell, J. Amer. Chem. Soc. 138 (2016) 4739–4756.
[24] A. Janda, B. Vlaisavljevich, L.-C. Lin, S. Mallikarjun Sharada, B. Smit, M. Head-Gordon, A.T. Bell, J. Phys. Chem. C 119 (2015) 10427–10438.
[25] T.J.H. Vlugt, E. García-Pérez, D. Dubbeldam, S. Ban, S. Calero, J. Chem. Theory Comput. 4 (2008) 1107–1118.
[26] R.B. Getman, Y.-S. Bae, C.E. Wilmer, R.Q. Snurr, Chem. Rev. 112 (2012) 703–723.
[27] Z. Qiao, A. Torres-Knoop, D. Dubbeldam, D. Fairen-Jimenez, J. Zhou, R.Q. Snurr, AIChE J. 60 (2014) 2324–2334.
[28] Z.R. Herm, B.M. Wiers, J.A. Mason, J.M. van Baten, M.R. Hudson, P. Zajdel, C.M. Brown, N. Masciocchi, R. Krishna, J.R. Long, Science 340 (2013) 960–964.
[29] J.J. Gutirrez-Sevillano, J.M. Vicent-Luna, D. Dubbeldam, S. Calero, J. Phys. Chem. C 117 (2013) 11357–11366.
[30] A. Poursaeidesfahani, A. Torres-Knoop, M. Rigutto, N. Nair, D. Dubbeldam, T.J. H. Vlugt, J. Phys. Chem. C 120 (2016) 1727–1738.
[31] D. Dubbeldam, S. Calero, D.E. Ellis, R.Q. Snurr, Mol. Sim. 42 (2015) 81–101.
[32] J.J. Potoff, J.I. Siepmann, AIChE J. 47 (2001) 1676–1682.
[33] M.G. Martin, J.I. Siepmann, J. Phys. Chem. B 102 (1998) 2569–2577.
[34] International Zeolite Association and Structure Commission and others, Database of zeolite structures, IZA Structure Commission, 2001.
[35] J.I. Siepmann, D. Frenkel, Mol. Phys. 75 (1992) 59–70.
[36] T.J.H. Vlugt, R. Krishna, B. Smit, J. Phys. Chem. B 103 (1999) 1102–1118.
[37] M. Laso, J.J. de Pablo, U.W. Suter, J. Comput. Phys. 97 (1992) 2817–2819.
[38] J. Houdayer, J. Comput. Phys. 116 (2002) 1783–1787.
[39] G.M. Torrie, J.P. Valleau, J. Comput. Phys. 23 (1977) 187–199.
[40] D. Dubbeldam, A. Torres-Knoop, K.S. Walton, Mol. Sim. 39 (2013) 1253–1292.
[41] T.J.H. Vlugt, R. Krishna, B. Smit, J. Phys. Chem. B 103 (1999) 1102–1118.
[42] X. Zhu, L. Wu, P.C. Magusin, B. Mezari, E.J. Hensen, J. Catal. 327 (2015) 10–21.
[43] E.J. Hensen, D.G. Poduval, D.M. Ligthart, J.R. van Veen, M.S. Rigutto, J. Phys. Chem. C 114 (2010) 8363–8374.
[44] D.W. Scott, J.P. McCullough, M.Z. El-Sabban, The Chemical Thermodynamic Properties of Hydrocarbons and Related Substances, US Government Printing Office, Washington, DC, 1974.
[45] E. Verheyen, C. Jo, M. Kurttepeli, G. Vanbutsele, E. Gobechiya, T.I. Korányi, S. Bals, G. Van Tendeloo, R. Ryoo, C.E. Kirschhock, J. Catal. 300 (2013) 70–80.